(15) G. K. Miner, T. P. Graham, and G. T. Johnston, *Rev. Sci. Instrum.*, **43**, 1297 (1972)
(16) I. B. Goldberg, unpublished research.
(17) J. R. Pilbrow and M. E. Winfield, *Mol. Phys.*, **25**, 1073 (1973).
(18) N. D. Chasteen, personal communication.
(19) P. C. Taylor and P. J. Bray, *J. Magn. Reson.*, **2**, 305 (1970).
(20) J.-L. Marill and D. Cornet, *J. Chim. Phys. Phys.-Chim. Biol.*, **70**, 336 (1973).
(21) N. M. Atherton, "Electron Spin Resonance", Hilger and Watts, London, 1973.
(22) K. V. S. Rao and M. C. R. Symons, *J. Chem. Soc. A*, 2163 (1971).
(23) P. W. Atkins and M. C. R. Symons, *J. Chem. Soc.*, 4363 (1964).
(24) S. P. Mishra and M. C. R. Symons, *J. Chem. Soc., Chem. Commun.*, 279 (1974).
(25) K. O. Christe, unpublished research.
(26) D. Lind, personal communication.
(27) K. Nishikida and F. Williams, *J. Am. Chem. Soc.*, **97**, 7166 (1975).
(28) N. Vanderkooi, J. S. MacKenzie, and W. B. Fox, *J. Fluorine Chem.*, **7**, 415 (1976).
(29) M. T. Rogers and L. D. Kispert, *J. Chem. Phys.*, **46**, 3193 (1967).
(30) J. E. Wertz and J. R. Bolton, "Electron Spin Resonance: Elementary Theory and Practical Applications", McGraw-Hill, New York, N.Y., 1972.
(31) S. P. So, *J. Chem. Phys.*, **67**, 2929 (1977).
(32) C. M. Hurd and P. Coodin, *J. Phys. Chem. Solids*, **28** 523 (1966).
(33) P. H. Kasai and E. B. Whipple, *Mol. Phys.*, **9**, 497 (1965).
(34) J. B. Farmer, M. C. L. Gerry, and C. A. McDowell, *Mol. Phys.*, **8**, 253 (1964).
(35) O. Edlund, A. Lund, M. Shiotani, J. Sohma, and K. A. Thuomas, *Mol. Phys.*, **32**, 49 (1976).
(36) K. O. Christe, R. D. Wilson, and C. J. Schack, *Inorg. Chem.*, **16**, 937 (1977).
(37) W. E. Tolberg, R. T. Rewick, R. S. Stringham, and M. E. Hill, *Inorg. Chem.*, **6**, 1156 (1967).

Contribution from Cattedra di Chimica Generale della Facoltà di Farmacia, the Istituto di Chimica Generale, and the Laboratorio CNR, Florence, Italy

Single-Crystal ESR Spectra of Copper(II) Complexes with Geometries Intermediate between a Square Pyramid and a Trigonal Bipyramid

ALESSANDRO BENCINI,[1a] IVANO BERTINI,*[1b] DANTE GATTESCHI,[1c] and ANDREA SCOZZAFAVA[1b]

Received March 30, 1978

The single-crystal ESR spectra of copper(II)-doped bis(*N*-methylsalicylaldiminato)zinc(II) and (bis(3-salicylaldiminatopropyl)methylamine)zinc(II) have been recorded. Both the complexes are five-coordinate with geometries intermediate between a square pyramid and a trigonal bipyramid. The g and A values of these complexes are discussed on the basis of an angular overlap model. Criteria are suggested for recognizing the ESR spectra of distorted five-coordinate complexes in diluted powders or frozen solutions.

Introduction

The ESR spectra of five-coordinate copper(II) complexes are now reasonably well understood as far as the two limiting square-pyramidal and trigonal-bipyramidal forms are concerned. The two forms can be easily recognized from the ESR spectra, since $g_\perp > g_\parallel \simeq 2.00$ and $|A_\parallel| \simeq |A_\perp| \simeq (60\text{–}100) \times 10^{-4}$ cm^{-1} for trigonal and $g_\parallel > g_\perp$ and $|A_\perp| \ll |A_\parallel| \simeq (120\text{–}150) \times 10^{-4}$ cm^{-1} for square-pyramidal complexes.[2-8] Also some magnetically undiluted complexes with intermediate geometries have been studied,[9-11] but no information is available on the values of the hyperfine coupling constants. Since five-coordinate complexes most commonly have geometries intermediate between the two limiting geometries,[12] is appeared interesting to us to study some model complexes in order to appreciate the pattern of variation of the spin-Hamiltonian parameters in passing from a pyramid to a bipyramid. We wish to report now the single-crystal ESR spectra of copper(II)-doped bis(*N*-methylsalicylaldiminato)zinc(II) (hereafter (Cu,Zn)SalMe)[13] and (bis(3-salicylaldiminatopropyl)methylamine)zinc(II) (hereafter (Cu,Zn)SalMeDPT)[14] (see the ligand structures below) and to compare the g and A values with a simple theoretical model which allows for the geometrical distortions from the idealized symmetry.

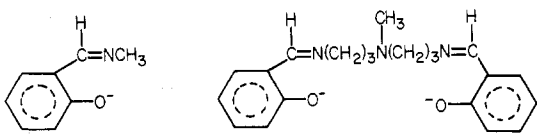

Experimental Section

All the compounds were prepared as previously described.[13,14] Single crystals of the copper doped into ZnSalMe and ZnSalMeDPT were obtained by slow evaporation of chloroform–benzene solutions. ZnSalMe crystallizes in the triclinic system: space group $P\bar{1}$; a = 9.48 Å, b = 10.53 Å, c = 8.45 Å, α = 99° 45′, β = 92° 58′, γ = 117° 58′; Z = 2.[15] The doped crystals were light green prisms with the (100) face most developed. ZnSalMeDPT crystals are monoclinic: space group $P2_1/c$; a = 6.913 Å, b = 13.975 Å, c = 19.893 Å, β = 91° 54′; Z = 4.[16] They were plates with the (001) face most prominent. Both types of crystals were oriented by Weissenberg techniques. The crystals were mounted on a Perspex cube, fitted to a Perspex rod. The morphological properties of the crystals were used to align them under a microscope. In the case of the monoclinic crystal the orientation was checked by the coincidence of the ESR signals of the two magnetically nonequivalent molecules in some particular orientation in the magnetic field. The ESR spectra were obtained using a Varian E-9 spectrometer equipped with X band. Three independent rotations along the three axes of the Perspex cube were performed. All of the spectra were recorded at liquid nitrogen temperature.

Results

(Cu,Zn)SalMe. The complex ZnSalMe is dimeric, formed by two trigonal-bipyramidal moieties sharing one axial and one equatorial ligand[15] (Figure 1). CuSalMe has a different coordination polyhedron but it assumes the same coordination as the zinc analogue when doped into the lattice of the latter compound.[17] Diluted solid solutions have been used in order to ensure that the coupling between the copper atoms is negligible; indeed no signal was observed in the spectra which could be attributed to directly interacting couples of copper atoms. The Z laboratory axis corresponds to the {010} direction whereas the X axis lies in the (010) plane making an angle of 9° 45′ with the $+c$ axis. In the rotation along the Y laboratory axis an extreme g value of 2.25 is found, which closely corresponds to the highest g value of the powder spectra (Figure 2). Also the value of the hyperfine coupling constant coincides with that of the powder spectra. The principal g values have been determined through the Ayscough method[18] and are shown in Table I, together with the coordinates of the points which identify the g_1, g_2, and g_3 directions in the triclinic unit cell. The g_2 and g_3 extremes were checked also by rotating around an axis parallel to the g_1 direction. The directions of

0020-1669/78/1317-3194$01.00/0

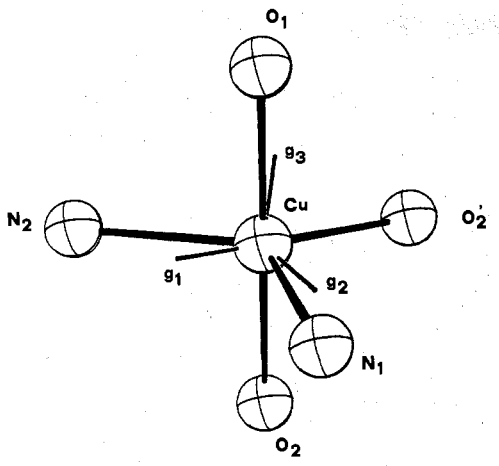

Figure 1. ORTEP drawing of CuSalMe chromophore showing the principal g directions.

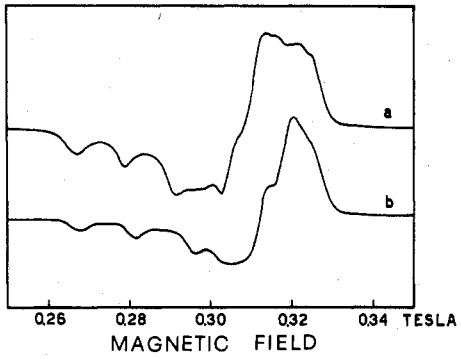

Figure 2. Polycrystalline powder spectra at liquid nitrogen temperature: (a) (Cu,Zn)SalMe; (b) (Cu,Zn)SalMeDPT.

Table I. ESR Parameters and g Directions for Two Complexes

	(Cu,Zn)SalMe	(Cu,Zn)SalMeDPT
g_1	2.25	2.23
g_2	2.13	2.07
g_3	2.02	2.04
A_1[a]	131	150
A_2[a]	65	38
A_3[a]	47	66
P_1[b]	0.0350, 0.2382, 0.1375[c]	0.0508, −0.0680, 0.3093[d]
P_2[b]	−0.0350, 0.1666, −0.0259[c]	−0.0810, 0.0099, 0.3110[d]
P_3[b]	0.1337, 0.2609, 0.0139[c]	0.1064, 0.0189, 0.3408[d]

[a] Expressed as $cm^{-1} \times 10^4$. [b] The P_i's represent the extremes of the unit vectors starting from the metal atom and parallel to the g_i main directions. [c] Triclinic coordinates. [d] Monoclinic coordinates.

the g axes relative to the molecular parameters are shown in Figure 1. The g_1 axis is practically parallel to the M–O_2' bond direction, while g_3 is quite close to the M–O_2 and M–O_1 bonds, which correspond to the trigonal axis of a bipyramid. The principal axes of the **A** tensor were found to be coincident with the axes of the **g** tensor within experimental error.

(Cu,Zn)SalMeDPT. The complex ZnSalMeDPT is monoclinic, $Z = 4$;[16] therefore two signals were present in the spectra obtained with the static magnetic field in the *ab* and *bc* planes. The extreme values in these rotations were determined and g_{ij}^2 were calculated by the method of Ayscough.[18] The principal values and directions of the **g** tensor, together with the coordinates of the points which identify the g_1, g_2, and g_3 directions in the monoclinic cell, are shown in Table I. In Table I are also shown the corresponding principal A values. Although the overlap of the signals prevented a detailed analysis of the angular dependence of the **A** tensor, there is some indication in the spectra that the principal axes of A are rotated by small angles from the principal directions of g. In Figure 3 are shown the orientations of the g axes within the molecular framework. The direction g_1 is practically coincident with the M–N_3 bond while g_3 is close to the M–N_2 bond, which should identify the trigonal axis of an idealized bipyramid. No ligand hyperfine splitting was observed for either complex under any condition.

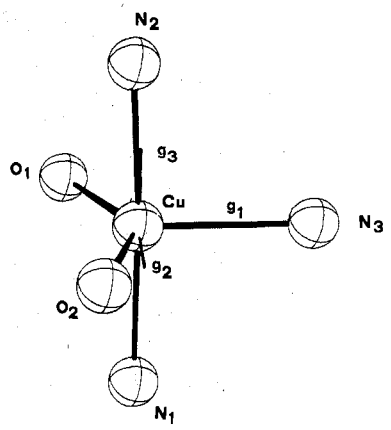

Figure 3. ORTEP drawing of CuSalMeDPT chromophore showing the principal g directions.

Discussion

Both complexes show distorted geometries intermediate between a trigonal bipyramid and a square pyramid. Since the copper atoms enter as a substitional impurity into the lattice of the zinc analogue, some distortions of the coordination polyhedron cannot be excluded. However, the principal g directions in both (Cu,Zn)SalMe (I) and (Cu,Zn)SalMeDPT (II) are close to the bond directions of the reported structures, suggesting that the distortions of the lattice induced by the copper ions, if any, are small. In both cases the smallest g value (g_3) is found close to the direction of the trigonal axis of a trigonal bipyramid. Passage from a bipyramid to a pyramid along the most symmetric path keeps the molecule in C_{2v} symmetry. Looking at the two chromophores of the compounds investigated, one can recognize that the C_2 axis of the C_{2v} symmetry might correspond to the M–O_2' direction in I and to the M–N_3 direction in II. In the limit of a regular square pyramid this axis should be the tetragonal axis. The angular distortions of the two chromophores from C_{2v} symmetry are less marked for II (two angles around the M–N_3 bond are 113 and 106° respectively (average 109.5°)), while they are more pronounced for I, the corresponding angles being 111 and 125° (average 118°). The two angles would be identical in C_{2v} symmetry. Despite these deviations, an attempt at rationalization of the present data may be based only on C_{2v} symmetry.

For this purpose it is possible to define a coordinate system as shown below.

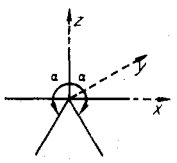

As α moves from 90 to 120°, the chromophore passes from a square pyramid to a trigonal bypyramid. The highest energy orbital in a ligand field formalism can be described as $(\cos \beta)|x^2 - y^2\rangle + (\sin \beta)|z^2\rangle$ where $\beta = 0°$ for $\alpha = 90°$ and $\beta = -30°$ for $\alpha = 120°$. Using an angular overlap approach[18-20] and typical parameters for e_σ and e_π, i.e. $e_\sigma = 3000$ cm^{-1} and $e_\pi = 0$ cm^{-1} for every ligand, we calculate the angular dependence of the energy levels as shown in Figure 4a. Using these results one can calculate expressions for g and A, as a function of α. The calculated expressions are shown in Table

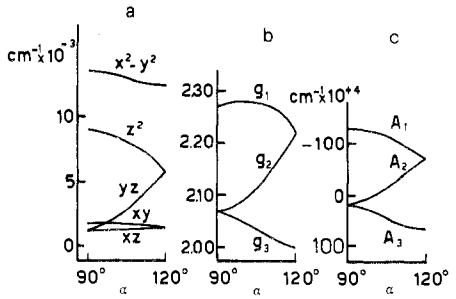

Figure 4. (a) Energy level diagram for the C_{2v} five-coordinate complex as a function of the angle α (see text); $e_\sigma = e_{\sigma'} = e_{\sigma''} = 3000$ cm^{-1}; $e_\pi = e_{\pi'} = e_{\pi''} = 0$. (b, c) Dependence of the g and A values on the angle α ($P = 0.024$ cm^{-1}, $K = 0.30$ cm^{-1}).

II where the γ_i's are the molecular orbital coefficients defined as shown below.

$$|1\rangle = \gamma_1(\cos\beta)|x^2 - y^2\rangle + (\sin\beta)|z^2\rangle$$
$$|2\rangle = \gamma_2(\sin\beta)|x^2 - y^2\rangle - (\cos\beta)|z^2\rangle$$
$$|3\rangle = \gamma_3|xz\rangle$$
$$|4\rangle = \gamma_4|yz\rangle$$
$$|5\rangle = \gamma_5|xy\rangle$$

By inspection it is easy to verify that for $\beta = 0$ and $-30°$ the formulas of Table II reduce to the reported expressions for C_{4v} and D_{3h} symmetries, respectively.[2,7]

In Figure 4b,c the calculated variations of g and A as a function of the angle α are shown. The input energy differences were those of the calculations of the energy levels of Figure 4a, and the other parameters were those indicated in the caption of the figure. The delocalization of the unpaired electron onto the ligand has been taken into account by using a ξ value reduced 20% as compared to the free-ion value. A more detailed study of the covalency effects is outside the scope of this work; however, the pattern of g and A values shown in Figure 4b,c appears to be largely insensitive to different reduction factors. The g_z and g_x values are expected to be not too largely affected by the variation of α while g_y is the most highly affected. For example, g_x is calculated as 2.00 in the limit of D_{3h} symmetry and as 2.07 in the limit of tetragonal symmetry. Both the calculated values compare well with the values reported for trigonal and tetragonal copper(II) complexes;[2-8] g_z varies from 2.22 to 2.27 again comparing well with the values found for $g_\perp$ of trigonal-bipyramidal complexes and for $g_\parallel$ of tetragonal complexes.[2-8]

A somewhat similar pattern is expected for A with A_1 varying from -130×10^{-4} cm^{-1} in the limit of tetragonal symmetry to -70×10^{-4} cm^{-1} in the limit of trigonal symmetry, and A_3 varies correspondingly from $+20 \times 10^{-4}$ to $+60 \times 10^{-4}$ cm^{-1}. Again A_2 is the most highly affected in this case changing also sign on passing from tetragonal to trigonal symmetry.

Going back again to the experimental values of Table I one sees the remarkable fact that the principal directions of the **g** tensors correspond to the x, y, and z axes of C_{2v} treatment, encouraging therefore the use of such an idealized symmetry, notwithstanding the actual low symmetry of the complexes. If in Table I the substitutions $1 \rightarrow z$, $2 \rightarrow y$, and $3 \rightarrow x$ are performed, the experimental data can be directly compared to the calculated values of Figure 4. In I the g value pattern is completely anisotropic while the A values are all relatively large and at least measurable. The smallest g value is observed parallel to the trigonal axis and the largest g value is parallel to Z in very good agreement with the pattern shown in Figure 4b. Similar also is the behavior of II with the difference that now g_y is smaller than in I, 2.07 against 2.13. These results suggest that II is closer to the tetragonal limit while I is closer to the trigonal limit. As a matter of fact the X-ray structure data available for the zinc analogue of I[14] and the nickel analogue of II[16] yield average α values of 118 and 109.5°, respectively, in accord with the above conclusions. Also the pattern of the A values can be considered to conform to this view, A_y being smaller in II than in I, as can be expected according to the pattern of Figure 4c.

Table II. Expressions for the g and A Tensors in C_{2v} Symmetry[a]

$$g_{xx} = \frac{2\gamma_1\gamma_4(\cos\beta + 3^{1/2}\sin\beta)^2\xi}{\Delta_{yz}}$$

$$A_{xx} = P\left[-K\gamma_1^2 + \frac{2}{7}\gamma_1^2((\cos 2\beta) - 3^{1/2}\sin 2\beta) + \frac{2(3^{1/2})}{7}\gamma_1^2\gamma_5^2(\sin 2\beta)\frac{\xi}{\Delta_{xy}} - \frac{3}{7}\gamma_1^2\gamma_3^2((\cos 2\beta) - \frac{3^{1/2}}{3}\sin 2\beta)\frac{\xi}{\Delta_{xz}} + 2\gamma_1^2\gamma_4^2\frac{\xi}{\Delta_{yz}}((\cos\beta) + 3^{1/2}\sin\beta)^2\right]$$

$$g_{yy} = \frac{2\gamma_1\gamma_3((\cos\beta) - 3^{1/2}\sin\beta)^2\xi}{\Delta_{xz}}$$

$$A_{yy} = P\left[-K\gamma_1^2 + \frac{2}{7}\gamma_1^2((\cos 2\beta) + 3^{1/2}\sin 2\beta) - \frac{2(3^{1/2})}{7}\gamma_1^2\gamma_5^2(\sin 2\beta)\frac{\xi}{\Delta_{xy}} - \frac{3}{7}\gamma_1^2\gamma_4^2((\cos 2\beta) + \frac{3^{1/2}}{3}\sin 2\beta)\frac{\xi}{\Delta_{yz}} + 2\gamma_1^2\gamma_3^2\frac{\xi}{\Delta_{xz}}((\cos\beta) - 3^{1/2}\sin\beta)^2\right]$$

$$g_{zz} = \frac{8\gamma_1\gamma_5\cos^2\beta}{\Delta_{xy}}$$

$$A_{zz} = P\left[-K\gamma_1^2 - \frac{4}{7}\gamma_1^2(\cos 2\beta) + \frac{3}{7}\gamma_1^2\gamma_4^2((\cos 2\beta) + \frac{3^{1/2}}{3}\sin 2\beta)\frac{\xi}{\Delta_{yz}} + \frac{3}{7}\gamma_1^2\gamma_3^2\frac{\xi}{\Delta_{xz}}((\cos 2\beta) - \frac{3^{1/2}}{3}\sin 2\beta) + 8\gamma_1^2\gamma_5^2(\cos^2\beta)\frac{\xi}{\Delta_{xy}}\right]$$

[a] β and the γ_i's are defined in the text. The Δ_i's are the energy separation of the ground and the indicated orbital. $P = 2g_N\beta_N\beta_0\langle 1/r^3\rangle$ where β_0 is the Bohr magneton, β_N is the nuclear magneton, g_N is the nuclear g factor, and r is the distance between the electron and the nucleus. K accounts for the contribution which brings the contact interaction into the value for the hyperfine splitting.

Conclusions

The analysis of the spin-Hamiltonian parameters of five-coordinate complexes with geometries intermediate between the extremes of a square pyramid and a trigonal bipyramid have shown some characteristics which are substantially different from those of copper(II) ions in other stereochemistries. For instance it is well-known that tetragonal copper(II) complexes are characterized by $g_\parallel > g_\perp$, large $A_\parallel$, and $A_\perp$ often hard to extract from the complicated shape of the perpendicular region of a powder spectrum.[2,3,22] Intermediate five-coordinate copper complexes seem now to be characterized by strong rhombic distortions with one g value smaller than 2.04 and by A values which are all measurable. These characteristics show up neatly in the single-crystal spectra, although they may not be straightforwardly recognized

in the powder spectra (see Figure 2). However, it can be noted that while the low-field region of powder spectra resembles the usual tetragonal copper(II) spectra, the high-field region is more spread out in the case of the intermediate five-coordinate complexes, as a consequence of both the anisotropy in the g values and the relatively large values of A.

Registry No. CuSalMe, 19031-10-8; ZnSalMe, 16457-01-5; CuSalMeDPT, 15378-53-7; ZnSalMeDPT, 15412-50-7.

References and Notes

(1) (a) Laboratorio CNR. (b) Cattedra di Chimica Generale della Facoltà di Farmacia. (c) Istituto di Chimica Generale.
(2) B. J. Hathaway and D. E. Billing, *Coord. Chem. Rev.*, **5**, 143 (1970).
(3) B. A. Goodman and J. B. Raynor, *Adv. Inorg. Chem. Radiochem.*, **13**, 135 (1970).
(4) B. J. Hathaway, D. E. Billing, R. J. Dudley, R. J. Fereday, and A. A. G. Tomlinson, *J. Chem. Soc. A*, 806 (1970).
(5) G. A. Jenynkova, I. D. Mikhein, and K. I. Zamaraev, *J. Struct. Chem. (Engl. Transl.)*, **11**, 18 (1970).
(6) R. Barbucci and M. J. Campbell, *Inorg. Chim. Acta*, **15**, L 15 (1975).
(7) R. Barbucci, A. Bencini, and D. Gatteschi, *Inorg. Chem.*, **16**, 2117 (1977).
(8) Actually copper doped into the tetragonal-pyramidal bis(benzoylacetonato)zinc monoethanolate show an $A_{\parallel}$ value of 182×10^{-4} cm^{-1}: R. L. Belford and D. C. Duan, *J. Magn. Reson.*, **29**, 293 (1978).
(9) A. Bencini and D. Gatteschi, *Inorg. Chem.*, **16**, 1994 (1977).
(10) D. M. L. Goodgame and G. Brun, *Bull. Soc. Chim. Fr.*, **7**, 2236 (1973).
(11) J. R. Wasson, D. K. Klassen, H. W. Richardson, and W. E. Hatfield, *Inorg. Chem.*, **16**, 1906 (1977).
(12) R. Morassi, I. Bertini, and L. Sacconi, *Coord. Chem. Rev.*, **11**, 343 (1973).
(13) L. Sacconi, M. Ciampolini, F. Maggio, and G. Del Re, *J. Am. Chem. Soc.*, **82**, 815 (1960).
(14) L. Sacconi and I. Bertini, *J. Am. Chem. Soc.*, **88**, 5180 (1966).
(15) P. L. Orioli, M. Di Vaira, and L. Sacconi, *Inorg. Chem.*, **5**, 400 (1966).
(16) M. Di Vaira, P. L. Orioli, and L. Sacconi, *Inorg. Chem.*, **10**, 553 (1971). The structure was solved for the nickel(II) derivative of which the zinc analogue is isomorphous.
(17) L. Sacconi, M. Ciampolini, and G. P. Speroni, *J. Am. Chem. Soc.*, **87**, 3102 (1965).
(18) P. B. Ayscough, "Electron Spin Resonance in Chemistry", Methuen, London, 1967.
(19) C. E. Schäffer, *Struct. Bonding (Berlin)*, **14**, 69 (1973).
(20) D. W. Smith, *Struct. Bonding (Berlin)*, **12**, 49 (1972).
(21) I. Bertini, D. Gatteschi, and A. Scozzafava, *Isr. J. Chem.*, **15**, 189 (1977).
(22) G. Formicka-Kozlowska, H. Kozlowski, and B. Jezowska-Trzebiatowska, *Inorg. Chim. Acta*, **24**, 1 (1977).

Contribution from the Department of Chemistry, Purdue University, West Lafayette, Indiana 47907

Studies on Metal Carboxylates. 14.[1] Reactions of Molybdenum(II) and Rhenium(III) Carboxylates with the Gaseous Hydrogen Halides in Alcoholic Media. Synthesis, Characterization, and Reactivity of the New Haloanions of Molybdenum and Rhenium, $Mo_2Br_6^-$, $Mo_4I_{11}^{2-}$, and $Re_2I_8^{2-}$

H. D. GLICKSMAN and R. A. WALTON*

Received April 27, 1978

The reactions of the molybdenum(II) and rhenium(III) carboxylates with hydrogen bromide and hydrogen iodide in alcoholic media are quite different from those previously encountered in the analogous reactions of these complexes with the gaseous hydrogen halides. The salts $(Bu_4N)Mo_2Br_6$ and $(Bu_4N)_2Mo_4I_{11}$ are produced when HBr and HI are reacted with methanol solutions containing $Mo_2(O_2CCH_3)_4$ and the appropriate tetra-*n*-butylammonium halide. While the paramagnetic iodide salt (μ_{eff} = 1.95 μ_B and g_{av} = 2.03 at room temperature) is known to contain a tetrahedral Mo_4 cluster, the detailed structure of $(Bu_4N)Mo_2Br_6$ is unknown at present although it almost certainly contains, as its most dominant structural feature, pairs of molybdenum atoms bound together by a very strong metal–metal bond. A discrete $Mo_2Br_6^-$ anion with an "ethane-like" structure would possess a $\sigma^2\pi^4(\pi^*)^1$ ground-state electronic configuration and a metal–metal bond order of 2.5. $(Bu_4N)Mo_2Br_6$ is paramagnetic (μ_{eff} = 1.5 μ_B and g_{av} = 1.98 at room temperature) and reacts with pyridine and tertiary phosphines (PEt_3, P-*n*-Pr_3, $Ph_2PCH_2CH_2PPh_2$, and $Ph_2PCH_2CH_2AsPh_2$) to afford the molybdenum(II) dimers $Mo_2Br_4L_4$ and $Mo_2Br_4(LL)_2$. These reactivity patterns are quite different from those displayed by $(Bu_4N)_2Mo_4I_{11}$ toward these same ligands. The treatment of mixtures of $Re_2(O_2CC_6H_5)_4Cl_2$ and Bu_4NX with HX (X = Cl, Br, or I) in methanol or ethanol affords the salts $(Bu_4N)_2Re_2X_8$. This is the first reported synthesis of the octaiododirhenate(III) anion, a species which upon reaction with tertiary phosphines produces the rhenium(II) dimers $Re_2I_4(PR_3)_4$, where R = Et, *n*-Pr, or *n*-Bu, and $Re_2I_4(LL)_2$, where LL = $Ph_2PCH_2CH_2PPh_2$ or $Ph_2PCH_2CH_2AsPh_2$. The reaction of $(Bu_4N)_2Re_2I_8$ with acetic and pivalic acids leads to the carboxylate-bridged dimers $Re_2(O_2CR)_4I_2$. When a methanol solution of $Re_2(O_2CC_6H_5)_4Cl_2$ is reacted with HCl in the absence of Bu_4N^+, the green methyl benzoate complex $Re_2Cl_6(C_6H_5CO_2CH_3)$ is formed. This species is probably the final reaction intermediate prior to the formation of $(Bu_4N)_2Re_2Cl_8$ when an excess of Bu_4N^+ is added.

Introduction

The reactions of crystalline molybdenum(II) acetate with *gaseous* hydrogen chloride, bromide, and iodide at ca. 300 °C produces the molybdenum(II) halides, β-MoX_2,[1-4] which are the parent halides of the haloanions $Mo_2X_8^{4-}$,[5-7] and, accordingly, are best formulated as $[Mo_2X_4]_n$.[1,4] The analogous metal–metal bonded rhenium(III) acetate, $Re_2(O_2CCH_3)_4Cl_2$, also reacts upon treatment with the gaseous hydrogen halides but, in this instance, a trinuclear halide cluster Re_3X_9, where X = Cl, Br, or I, is produced.[1,4] Since $Mo_2(O_2CCH_3)_4$ and $Re_2(O_2CCH_3)_4Cl_2$ are converted to salts of the $Mo_2Cl_8^{4-}$ and $Re_2Cl_8^{2-}$ anions upon treatment with concentrated hydrochloric acid,[5,8,9] the course of the reactions between these dimeric metal–metal bonded acetates and HX is clearly dependent upon the reaction conditions. The possibility that the reactions in aqueous media could differ significantly from those which might occur when a nonaqueous solvent system was used prompted us to explore the reactions of $Mo_2(O_2CCH_3)_4$ and $Re_2(O_2CC_6H_5)_4Cl_2$ with the hydrogen halides in alcoholic media (methanol and ethanol). This study has led, among other things, to the isolation of salts of the new $Mo_2Br_6^-$, $Mo_4I_{11}^{2-}$, and $Re_2I_8^{2-}$ anions. In the present article we describe details of their synthesis, characterization, and reactivity.

Experimental Section

Starting Materials. The following compounds were prepared by standard literature procedures: $Mo_2(O_2CCH_3)_4$,[2,10] $Re_2(O_2CCH_3)_4Cl_2$,[4,11] and $Re_2(O_2CC_6H_5)_4Cl_2$.[12] Reagent grade solvents and gases were obtained from commercial sources. All solvents were

0020-1669/78/1317-3197$01.00/0